



ORIGINAL ARTICLE

Mannose and phosphomannose isomerase regulate energy metabolism under glucose starvation in leukemia

Yusuke Saito¹  | Mariko Kinoshita¹ | Ai Yamada¹ | Sayaka Kawano¹ |
 Hong-Shan Liu¹ | Sachiyo Kamimura¹ | Midori Nakagawa¹ | Syun Nagasawa¹ |
 Tadao Taguchi² | Shuhei Yamada³ | Hiroshi Moritake¹ 

¹Division of Pediatrics, Faculty of Medicine, University of Miyazaki, Miyazaki, Japan

²Center for the Development of Pharmacy Education, Faculty of Pharmacy, Meijo University, Nagoya, Japan

³Department of Pathobiochemistry, Faculty of Pharmacy, Meijo University, Nagoya, Japan

Correspondence

Yusuke Saito, Division of Pediatrics, Faculty of Medicine, University of Miyazaki, Kiyotake, Japan.

Email: yusuke_saitoh@med.miyazaki-u.ac.jp

Funding information

JSPS KAKENHI, Grant/Award Number: JP 18K16094, JP19K17367 and JP 20K08735; Shinnihon Foundation of Advanced Medical Treatment Research; Japanese Society of Hematology Research

Abstract

Diverse metabolic changes are induced by various driver oncogenes during the onset and progression of leukemia. By upregulating glycolysis, cancer cells acquire a proliferative advantage over normal hematopoietic cells; in addition, these changes in energy metabolism contribute to anticancer drug resistance. Because leukemia cells proliferate by consuming glucose as an energy source, an alternative nutrient source is essential when glucose levels in bone marrow are insufficient. We profiled sugar metabolism in leukemia cells and found that mannose is an energy source for glycolysis, the tricarboxylic acid (TCA) cycle, and the pentose phosphate pathway. Leukemia cells express high levels of phosphomannose isomerase (PMI), which mobilizes mannose to glycolysis; consequently, even mannose in the blood can be used as an energy source for glycolysis. Conversely, suppression of PMI expression or a mannose load exceeding the processing capacity of PMI inhibited transcription of genes related to mitochondrial metabolism and the TCA cycle, therefore suppressing the growth of leukemia cells. High PMI expression was also a poor prognostic factor for acute myeloid leukemia. Our findings reveal a new mechanism for glucose starvation resistance in leukemia. Furthermore, the combination of PMI suppression and mannose loading has potential as a novel treatment for driver oncogene-independent leukemia.

KEYWORDS

activation and metabolism of carcinogens, hematopoietic organ, leukemia metabolism, glycolysis, mannose metabolism

1 | INTRODUCTION

Leukemia cell proliferation requires activation and reprogramming of metabolic pathways to supply anabolic cell growth. This aberrant cancer metabolism was first recognized by Warburg,¹ who postulated that cancer tissues have a higher rate of glucose uptake and glycolysis compared with normal tissues and rely primarily on

glucose to produce ATP with or without oxygen. Oncogenic driver genes regulate metabolic pathways such as MYC and RAS, which drive metabolic reprogramming in leukemia. Elevated MYC expression is a hallmark of Burkitt's lymphoma and acute lymphoblastic leukemias (ALL). Aberrant activation of MYC leads to increased glucose uptake and glycolytic activity, glutaminolysis, and lipid synthesis.²⁻⁵ Activating mutations in the RAS pathway are characteristic of

This is an open access article under the terms of the Creative Commons Attribution-NonCommercial License, which permits use, distribution and reproduction in any medium, provided the original work is properly cited and is not used for commercial purposes.

© 2021 The Authors. *Cancer Science* published by John Wiley & Sons Australia, Ltd on behalf of Japanese Cancer Association.

juvenile myelomonocytic leukemia,⁶ ALL, and acute myeloid leukemia (AML)^{7,8}; RAS mutations increase glucose uptake and expression of glycolytic enzymes and promote a shift to anabolic metabolism.⁹ Furthermore, glycolytic activation is essential not only for proliferation but also for development of leukemia. Depletion of either pyruvate kinase isozyme M2 or lactate dehydrogenase A in normal and malignant cells markedly decreases leukemia cell growth, but not normal hematopoiesis.¹⁰ The proliferation of leukemia cells accelerates glucose consumption, leading to glucose insufficiency in the bone marrow (BM),¹¹ but leukemia cells can survive under metabolic starvation. We hypothesized that leukemia cells use sugars other than glucose as a glycolytic energy source. Our experiments revealed that these cells metabolize mannose using phosphomannose isomerase (PMI), and that mannose is an energy source for glycolysis and oxidative phosphorylation (OXPHOS). Mannose is a monosaccharide incorporated into cells through glucose transporters.¹² In pancreatic cancer and colorectal cancer, which express a low level of PMI, dietary mannose inhibits cancer cell growth and increases chemosensitivity of cisplatin and doxorubicin.¹³ By contrast, leukemia cells express a high level of PMI, and the role of mannose metabolism in energy metabolism remains to be clarified.¹³

In this study, we found that mannose metabolism plays a critical role in the metabolic adaptation of leukemia cells in glucose starvation. Our findings suggest that PMI suppression and mannose overload represent promising therapeutic approaches for leukemia.

2 | MATERIALS AND METHODS

2.1 | Cell lines, reagents, and antibodies

MV4-11, MOLM-13, MOLM14, THP-1, U937, K562, and NB4 cells were cultured in RPMI1640 supplemented with 10% FCS. MV4-11 was purchased from ATCC (Manassas, VA) THP-1, U937, and K562 were purchased from JCRB Cell Bank (Japanese Collection of Research Bioresources Cell Bank). MOLM13 and MOLM14 were kind gifts from Dr. Yusuke Furukawa (Jichi Medical University, Japan). Detailed information about these cell lines has been published previously.^{14,15} Proliferation of leukemia cells was measured using a Cell Counting Kit-8 (Dojindo Molecular Technologies).

Control CD34⁺ cells were purchased from STEMCELL Technologies. Reagents used in the study included the Carbohydrate Kit, D-(-)-tagatose, D-sorbitol, xylitol, D-mannose 6-phosphate sodium salt (Sigma-Aldrich), anti-AMPK α antibody (2532), and anti-phospho-AMPK α (Thr172) antibody (2535) (Cell Signaling Technologies).

2.2 | Patient samples

BM samples were obtained from patients with AML or ALL treated at the University of Miyazaki (Table S1). The study was approved by the Institutional Review Board of the Faculty of Medicine of the University of Miyazaki.

2.3 | Measurement of extracellular acidification rate

Extracellular acidification rate (ECAR) was measured using an XFp analyzer (Agilent Technologies). Leukemia cells were suspended in XF Assay Medium supplemented with 2 mM glutamine and seeded at 100 000 cells per well in a culture plate precoated with Cell-Tak (Thermo Fisher Scientific). The plate was centrifuged, left to equilibrate for 60 min in a CO₂-free incubator, and then transferred to the XFp analyzer. The Glycolysis Stress Test was performed as follows: (a) carbohydrates were injected to measure glycolysis; (b) oligomycin (1 μ mol/L) was added to measure glycolytic capacity and glycolytic reserve; and (c) 2-DG was applied to measure non-glycolytic acidification. Glycolytic activity was calculated as ECAR glycolysis/ECAR baseline.

2.4 | Measurement of oxygen consumption rate

Oxygen consumption rate (OCR) was also measured using the XFp analyzer. Leukemia cells were suspended in XF Assay Medium supplemented with 10 mmol/L glucose, 1 mmol/L pyruvate, and 2 mmol/L glutamine. Cells were seeded at 100 000 cells per well in a culture plate precoated with Cell-Tak. The plate was centrifuged, left to equilibrate for 60 min in a CO₂-free incubator, and then transferred to the XFp analyzer. The Mito Stress Test was performed as follows: (a) basal respiration was measured in XF Base Medium (1 mmol/L sodium pyruvate, 10 mmol/L glucose, 2 mmol/L glutamine); (b) oligomycin (1 μ mol/L) was injected to measure respiration linked to ATP production; (c) the uncoupler carbonyl cyanide 4-(trifluoromethoxy) phenylhydrazone (FCCP, 1 μ mol/L) was added to measure maximal respiration; and (d) rotenone and antimycin A (0.5 μ mol/L each) were applied together to measure non-mitochondrial respiration.

2.5 | Lentiviral transduction of AML cells with shRNA

pLKO.1 puro was a kind gift from Dr. Bob Weinberg (Addgene plasmid # 8453). Control shRNA (scramble) was a kind gift from Dr. David Sabatini (Addgene plasmid # 1864). The sequences of the shRNA oligonucleotides are provided in the Extended Data Table. Plasmids pMD2.G-VSV-G and psPAX2-Gag-Pol were purchased from Addgene. On day 2 post-transduction, cells were selected by exposure to puromycin (1 μ g/mL; Sigma-Aldrich) for 4 d. Knockdown efficiency was analyzed by measuring PMI mRNA levels by quantitative PCR analysis on day 4.

2.6 | Quantitative real-time PCR

RNA was isolated from leukemia cells using TRI Reagent (Molecular Research Center). cDNA was synthesized using random primers and SuperScript VILO (Thermo Fisher Scientific). Quantitative PCR was performed using Step One Plus (Thermo Fisher Scientific). Primers are listed in Table S2.

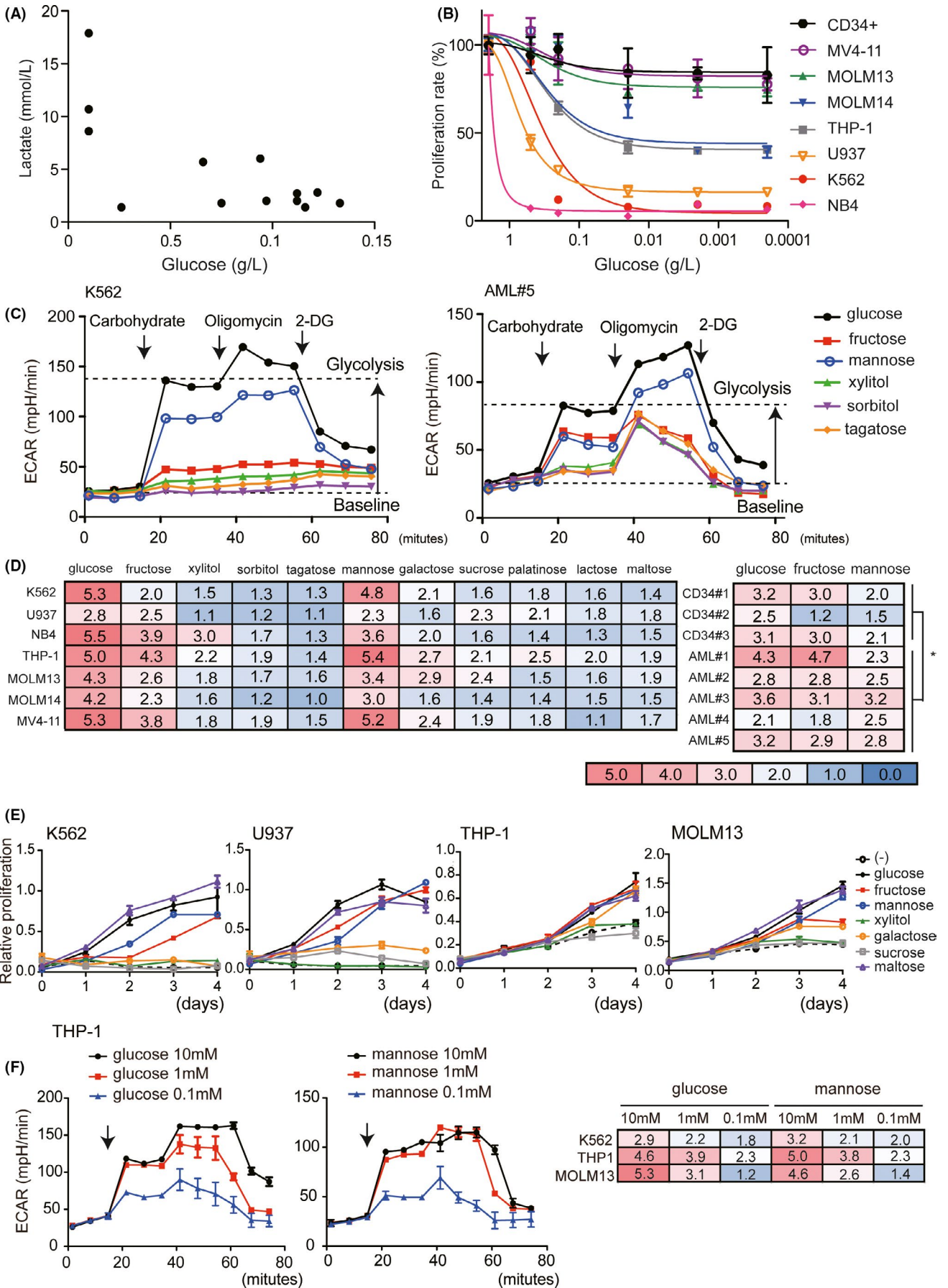


FIGURE 1 Leukemia cells utilize mannose and fructose as a glycolytic energy fuel under glucose-free conditions. (A) Bone marrow glucose and lactate concentration in leukemia patients. (B) Proliferation rates of leukemia cell lines under low-glucose condition. The proliferation rate at 2.0 g/L glucose was defined as 100%. (C) ECAR values of a leukemia cell line (K562) and patient sample (AML#5). The rate of change in ECAR before sugar addition (baseline) and after carbohydrate addition (glycolysis line) was measured on an extracellular flux analyzer. (D) Fold changes in ECAR (glycolytic activity) were normalized against glycolysis line with baseline. Glycolytic activity was calculated as ECAR glycolysis/ECAR baseline. Data are presented as means \pm standard deviation. * $P < .05$; ** $P < .01$; *** $P < .001$ (Student *t* test). (E) Proliferation curve of AML cell lines supplemented without (-) or with 10 mmol/L monosaccharides or disaccharides. (F) The rate of change in ECAR of leukemia cell lines (K562, THP-1, and MOLM13) in low concentrations of glucose and mannose

2.7 | Metabolome analyses

shScr and shPMI K562 cells were incubated for 6 h at 37°C in RPMI 1640 medium containing 10 mmol/L U-¹³C₆-mannose (Cambridge Isotope Laboratories) and 10% dialyzed FBS. Extracts were prepared from 10×10^6 cells with methanol containing internal standard solution (Human Metabolome Technologies). Cationic compounds and anionic compounds were measured on an Agilent CE-TOFMS system (Agilent) in positive mode.

2.8 | Measurement of plasma mannose

Mannose was assayed as previously described.¹⁶ Briefly, after samples were labeled with 4-aminobenzoyl ethyl ester, the concentration of mannose was determined by high-performance liquid chromatography.

2.9 | Retroviral BM transduction assays

pMIG-FLAG-MLL-AF9, was a kind gift from Daisuke Nakada (Addgene plasmid # 71443).¹⁷ pMSCV-BCR-ABL-IRES-GFP and pMSCV-NUP98-HOXA9 were kind gifts from Dr. Atsushi Hirao (Kanazawa University). G3T-hi cells (Takara Bio) were transiently transfected with MSCV vectors and the pCL-Eco retrovirus packaging vector using polyethylenimine (PEI). At day 4 post-injection of C57BL/6J with 5-fluorouracil (150 mg/kg; Kyowa Kirin, Japan), BM cells were harvested and incubated for 24 h in X-Vivo 15 (Lonza, Allendale, NJ) supplemented with 50 ng/mL SCF, 50 ng/mL TPO, 10 ng/mL IL-3, and 10 ng/mL IL-6 (all from Peprotech). After incubation, cells in plates coated with RetroNectin (Clontech) were spin infected (490 g for 45 min at 20°C) with retroviral supernatant supplemented with polybrene (8 μ g/mL). Next, 50 000 BM cells were then transplanted into lethally irradiated C57BL/6 mice. For secondary transplantations, GFP⁺ cells from primary recipient mice were transplanted into sublethally irradiated recipients.

2.10 | AML xenograft tumors

Female NOG mice (8 wk old) received a single subcutaneous injection of K562 cells (5×10^6) suspended in 100 μ l PBS mixed with an equal volume of Matrigel (BD Matrigel, BD Biosciences). Tumor growth was measured twice per week using calipers. Tumor volume was calculated using the modified ellipsoid formula: $1/2$ (length \times width²).

Mannose diet was manufactured by Research Diets Inc. All experiments were approved by the University of Miyazaki Animal Care and Use Committee.

2.11 | Colony-forming assay

Leukemia cells were plated in MethoCult M3234 (STEMCELL Technologies) medium supplemented with 20 ng/mL SCF, 10 ng/mL GM-CSF, 10 ng/mL IL-3, and 10 ng/mL IL-6 in accordance with the manufacturer's instructions.

2.12 | RNA sequencing (RNA-seq)

For RNA-seq experiments, poly(A)-selected libraries were prepared using the NEBNext Poly(A) mRNA Magnetic Isolation Module (NEB E7490) and NEBNext Ultra RNA Library Prep Kit for Illumina (E7530). All libraries were sequenced on an Illumina NovaSeq 6000 system using 2×150 bp paired-end sequencing. DESeq2 was used for data processing, normalization, and differential expression analysis.

RNA-seq data were deposited in the DNA Data Bank of Japan (accession number: DRA011988).

2.13 | Statistical analysis

Statistical analysis was performed using an unpaired Student *t* test or the log-rank test as appropriate. Calculations were performed using GraphPad Prism 8 software. Group data are expressed as means \pm standard deviation. Values of $P < .05$ were considered significant (* $P < .05$; ** $P < .01$; *** $P < .001$).

3 | RESULTS

3.1 | Leukemia cells use mannose as a glycolytic energy fuel under glucose starvation

To determine the degree of glucose starvation in the BM, we measured BM glucose and lactate concentrations in patients with AML or ALL. The glucose concentration was ≤ 0.5 g/L in four of 13 samples, and the lactate concentration was 5 mmol/L or more in 5 cases. These results indicated that proliferation of leukemia cells accelerates glucose consumption, leading to glucose insufficiency in some

FIGURE 2 PMI regulates mannose glycolytic metabolism in AML. (A) Peripheral blood (PB) or bone marrow (BM) plasma mannose concentration in paired samples acquired from 5 AML patients (AML#1, #3-6) at the time of diagnosis. (B) PB plasma mannose concentration of paired samples acquired from 6 AML patients (AML#2-7) at diagnosis and complete remission (CR). (C) Schematic outline of mannose metabolism. Mannose is taken up by GLUT-1 or GLUT-2 and phosphorylated rapidly by hexokinase (HK). Mannose-6-phosphate (Man-6-P) is converted to fructose 6-P-phosphate (Fru-6-P) by PMI, after which it enters glycolysis. Mannose can be used for glycosylation, and man-6-P also participates in biosynthesis of deaminoneuraminic acid (KDN). (D) Expression level of PMI in AML cells. Expression was normalized against the corresponding level of β -actin and the level in CD34⁺ cells. PMI expression and mannose metabolism activity were correlated. (E) Proliferation of K562 cells transduced with shScr or shPMI#1/#2 in medium containing 10 mmol/L glucose or 10 mmol/L mannose. Proliferation of K562 (F) and THP-1 (G) transduced with shScr or shPMI#1 in medium containing 10 mmol/L glucose, 10 mmol/L mannose, or both. AML cells transduced with shPMI exhibited significantly suppressed cell proliferation after addition of mannose. ECAR of K562 (H) and THP-1 (I) transduced with shScr and shPMI#1 upon addition of 10 mmol/L glucose or 10 mmol/L mannose. Addition of mannose reduced ECAR in shPMI AML cells. All data represent means \pm standard deviation. * $P < .05$; ** $P < .01$; *** $P < .001$ (Student *t* test)

samples (Figure 1A). In fact, glucose levels are significantly lower in leukemia BM than in peripheral blood.^{11,17} Next, we investigated whether leukemia cells could survive in a low-glucose environment. After 48 h in low-glucose medium, the numbers of MV4-11, MOLM13, and MOLM14 cells were $\geq 80\%$ of their numbers in normal medium. By contrast, the numbers of K562, U937, and NB4 were $< 50\%$ of their numbers in medium containing 1 g/L glucose or less (Figure 1B).

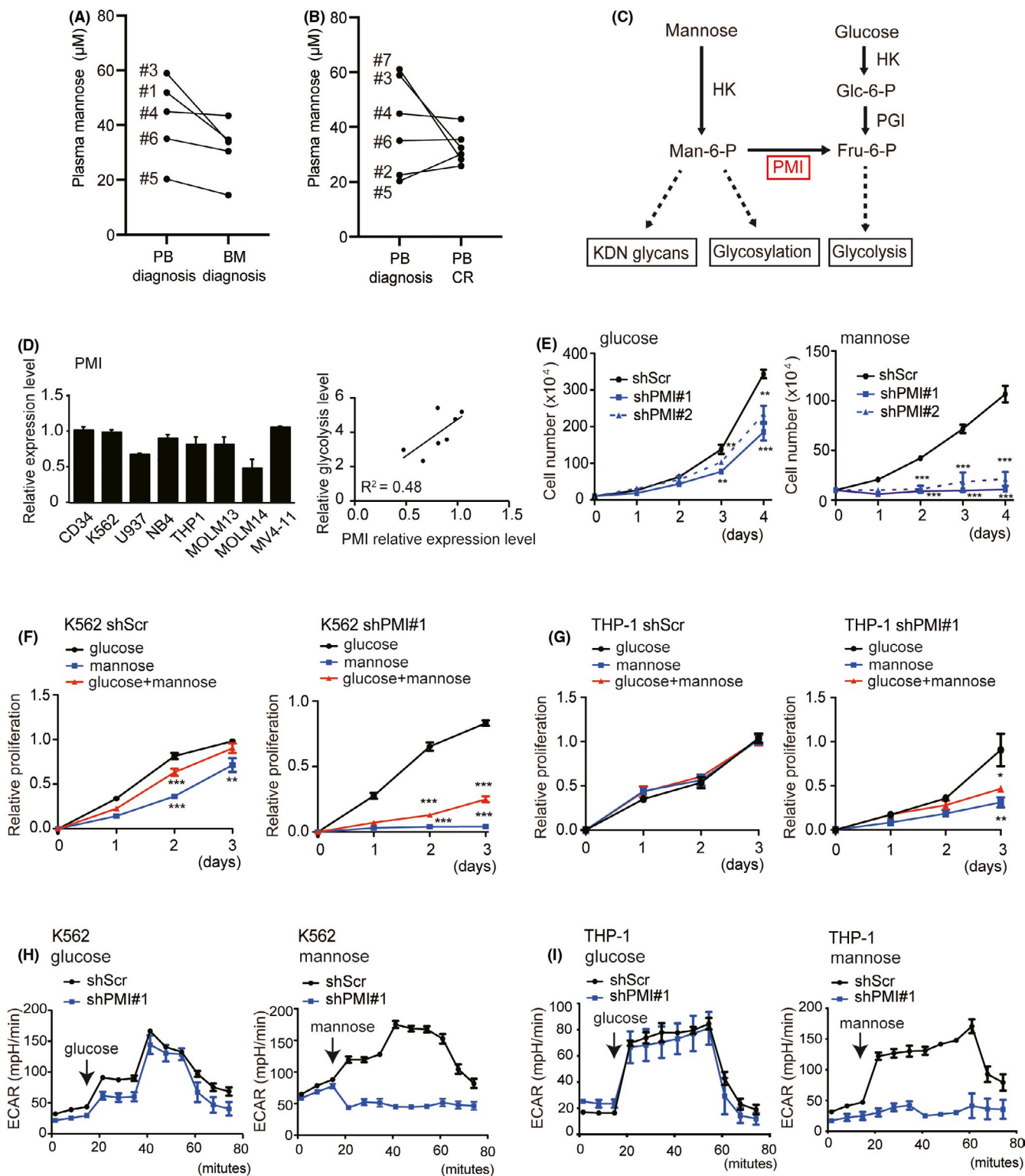
We hypothesized that leukemia cells vulnerable to glucose starvation maintained glycolysis using saccharides other than glucose to survive in the BM environment. To identify sugars that leukemia cells can use as an energy source for glycolysis, we measured the rate of change in ECAR before (baseline) and after sugar addition (glycolysis line) using an extracellular flux analyzer. In the presence of glucose, fructose, and mannose, all myeloid leukemia cell lines resulted in a 2–5-fold increase in ECAR, which specifically reflects the rate of glycolysis. Xylitol, galactose, and sucrose increased ECAR 2–3-fold in some cell lines (Figure 1C). Addition of glucose, fructose, and mannose to AML and ALL samples (Table S1) increased ECAR 2–3-fold. Leukemia cells could utilize mannose as an energy source regardless of their lineage or driver oncogene. By contrast, CD34⁺ normal hematopoietic stem cells exhibited a mild increase of ECAR in mannose relative to glucose (Figures 1D and S1). We next examined the effect of other saccharides on the growth of leukemia cells. In addition to glucose and mannose, fructose and maltose increased the growth of AML cell lines (Figure 1E). These results revealed that leukemia cells can utilize the monosaccharides mannose and fructose as energy sources for glycolysis. Fructose is a nutrient source during glucose starvation and is involved in the malignancy of AML.^{18–20} Here, we demonstrated that another sugar, mannose, is metabolized in AML cells. In fact, mannose-activated glycolysis to the same extent as glucose, even at low concentrations (Figure 1F). Although mannose is present in human blood at concentrations less than 2% of the glucose concentration,²¹ leukemia cells can still metabolize this sugar.

3.2 | Mannose metabolism in AML depends on PMI expression

In all samples, mannose concentration in BM containing many leukemia cells was lower than the concentration in peripheral blood

(Figure 2A). Mannose concentration did not significantly differ between samples taken at diagnosis and complete remission (Figure 2B). Mannose is taken up by GLUT-1 or GLUT-2 and phosphorylated rapidly by hexokinase (HK). Mannose-6-phosphate (Man-6-P) is converted to fructose 6-P-phosphate (Fru-6-P) by PMI, at which point it joins glycolysis (Figure 2C).¹² We analyzed the expression of HK and PMI in AML cell lines. PMI was expressed in all leukemia cell lines and positively correlated with mannose metabolic activity (Figures 2D and S2A).

PMI expression was significantly higher in AML samples (AML #1–#6) than in CD34⁺ normal hematopoietic stem cells (CD34 #1–#3; Figure S2B). Next, we knocked down the gene that encodes PMI in the AML cell lines K562 and THP-1 (Figure S2C). Two shRNA clones against PMI (clone 1 and 2; shPMI#1 and shPMI#2) induced mild growth inhibition in glucose medium relative to the shScramble control (shScr). Furthermore, proliferation of shPMI AML was completely suppressed in mannose medium (Figure 2E). Interestingly, in AML cells transduced with shPMI, cell proliferation was significantly suppressed by addition of mannose even in the presence of glucose (Figure 2F,G). To directly access glycolytic activity, we analyzed ECAR of shPMI AML cells following addition of glucose or mannose. Following addition of glucose, ECAR was mildly elevated in shPMI cells relative to shScr cells. By contrast, the addition of mannose decreased ECAR in shPMI cells (Figure 2H,I). These findings suggested that glucose metabolism is inhibited by mannose loading in PMI-suppressed AML cells. To analyze mannose metabolism in AML cells in detail, we performed additional ¹³C₆-mannose metabolic flux analysis. In PMI-expressing AML cells, mannose is metabolized to fuel glycolysis, the tricarboxylic acid (TCA) cycle, and the pentose phosphate pathway (PPP), ultimately producing ATP (Figure 3A). Conversely, in PMI-suppressed AML cells, Man-6-P accumulated, and the levels of glycolytic intermediates markedly decreased (Figure 3A). Furthermore, mannose treatment affected not only the levels of glycolytic intermediates, but also those of the TCA cycle and PPP metabolites (Figure 3A). Notably, levels of malic acid, fumaric acid, succinic acid derived from medium glutamine (M + 0), and ATP decreased, whereas levels of AMP increased, relative to those in shScr cells (Figure 3B). In addition, mannose induced AMPK phosphorylation relative to glucose-free medium (Figure S2D). Our results indicated that addition of mannose to PMI-suppressed AML cells suppressed not only glycolysis but also the TCA cycle and PPP, thereby inhibiting cell proliferation.



3.3 | Mannose diet changes hematopoiesis

In previous studies, to analyze the effects of mannose on the immune system and tumors *in vivo*, mice were provided with mannose in their drinking water.^{13,21,22} We have developed a new diet in which sucrose was replaced with mannose to limit glucose intake from the diet (Table S3). Initially, we evaluated the effects of mannose

on hematopoiesis and metabolism in C57BL6 mice fed a mannose diet for 4 wk. Plasma mannose concentrations were significantly elevated in the mannose diet group (Figure S3A), and the mannose diet group gained more weight than the normal diet group (Figure S3B). We observed no significant differences in glucose, liver function, or lipids between the 2 groups (Table S4). In addition, although we observed no significant difference in BM cell numbers, the number

(A) (Glycolysis)

(PPP)

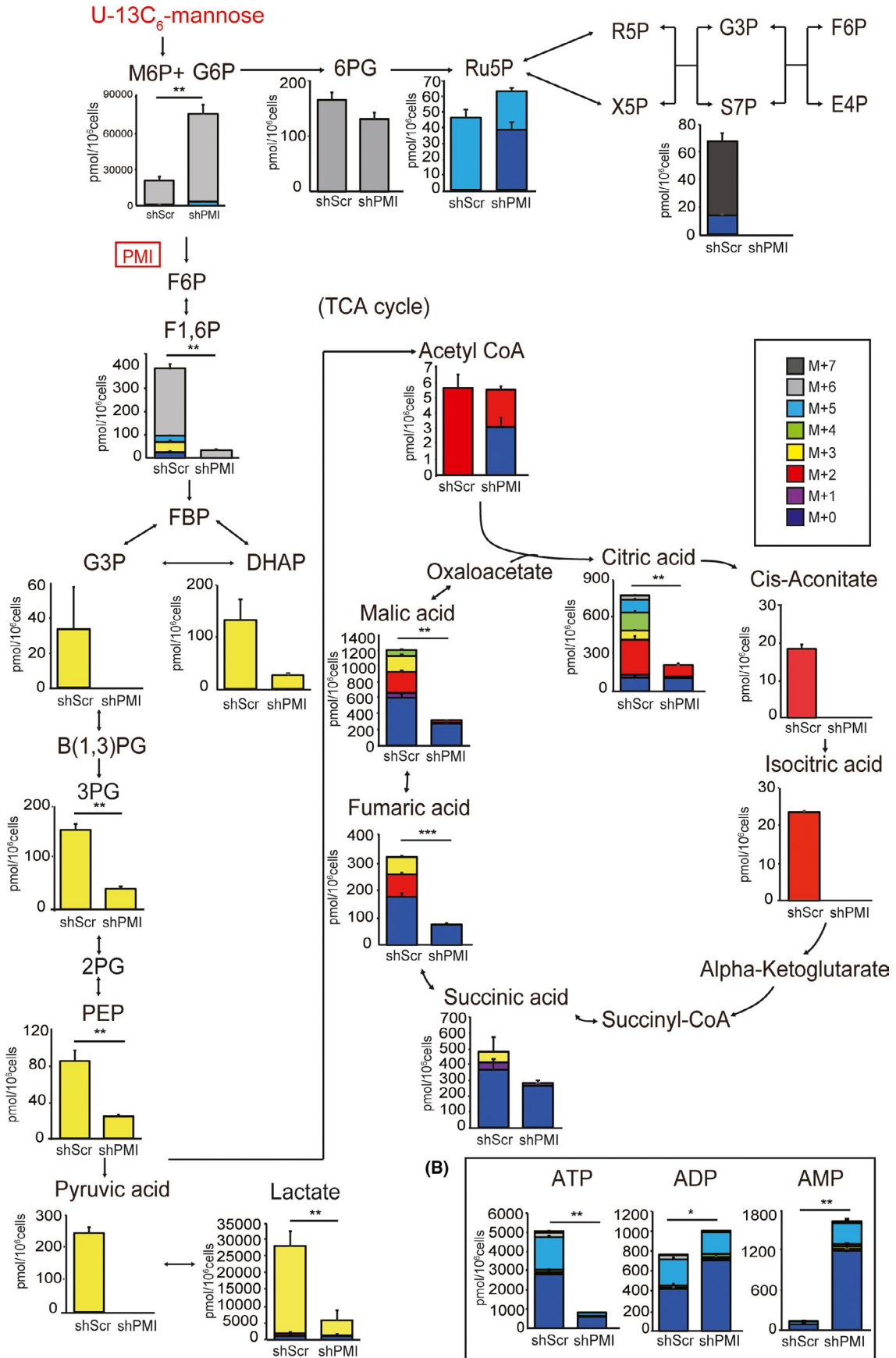


FIGURE 3 Addition of mannose to AML cells expressing low levels of PMI suppresses glycolysis, TCA cycle, and PPP. (A) Relative isotopolog distribution of glycolysis, TCA cycle, and PPP metabolites in K562 shScr or K562 shPMI cells, measured by CE-TOFMS after incubation for 6 h with 10 mmol/L U-¹³C₆-mannose (n = 3). (B) Relative isotopolog distribution of ATP, ADP, and AMP in K562 shScr or K562 shPMI cells, measured by CE-TOFMS after incubation for 6 h with 10 mmol/L U-¹³C₆-mannose (n = 3). Data are presented as means ± standard deviation. *P < .05; **P < .01; ***P < .001 (Student *t* test)

of LSK (lineage^{low}Sca-1⁺c-kit⁺) cells significantly decreased, whereas the number of GMP (lineage^{low}Sca-1⁻c-kit⁺CD16/32⁺CD34⁺) cells increased, in the mannose diet group relative to the normal diet group (Figure S3D,E). Mannose induces Treg cells in the immune system,²¹ and these findings show that a mannose diet directly affects the number of hematopoietic progenitor cells.

3.4 | A mannose diet that exceeds PMI capacity suppresses leukemia proliferation

We next examined the antileukemia effect of a mannose diet. shScr K562 or shPMI K562 cells were injected subcutaneously into the right dorsal of NOG mice, and mice harboring xenografts were fed a normal or mannose diet. Tumor growth was evaluated 15 d after injection (Figure 4A). The mannose diet did not affect growth of shScr K562 xenografts, but it did decrease both tumor volume and weight in shPMI K562 xenografts (Figure 4B–D). We next administered intravenously shScr K562 or shPMI K562 cells to NOG mice and examined the effect of low nutrient conditions on their proliferative potential in BM (Figure 4E). Peripheral blood chimerism on day 28 post-transplantation (Figure 4F) and BM (Figure 4G) showed a significantly lower percentage of CD71⁺ leukemic cells and longer survival in the shPMI K562 mannose diet group than in the other groups (Figure 4H). In the glucose-poor environment of BM, cell proliferation was more significantly inhibited by impaired mannose utilization. These results indicated that mannose loading that exceeds the processing capacity of PMI suppresses leukemia cell proliferation.

To determine whether PMI regulates energy metabolism in BM, we used a murine model in which blast crisis CML is driven by NUP98/HOXA9 and BCR-ABL,²³ and AML is driven by MLL-AF9^{16,24} (Figure 5A). PMI was highly expressed in murine blast crisis CML and AML cells relative to normal whole BM (WBM) cells (Figure S4A). Addition of mannose to murine leukemia cells increased ECAR 2-fold. By contrast, normal WBM cells and stem cell-enriched c-Kit-positive (c-kit⁺) exhibited a mild increase in mannose ECAR relative to leukemia cells (Figure 5B).

Next, we knocked down PMI in murine leukemia cells (Figure S4B). Colony-forming assays revealed that 2 shRNA clones against PMI (clone 1 and 2; shPmi#1 and shPmi#2) induced mild growth inhibition relative to shScr (Figure S4C). Furthermore, in blast crisis CML, addition of mannose reduced proliferation in shScr and shPmi cells (Figure 5C); this effect was more prominent in shPmi cells. In MLL-AF9 cells, addition of mannose decreased cell proliferation only in shPmi (Figure 5D). We next tested whether PMI inhibition would sensitize murine leukemia cells to a mannose diet by subjecting secondary recipient mice

to blast crisis CML. Strikingly, mannose diet extended the survival of mice transplanted with shScr and shPmi cells (Figure 5E), and significantly extended the survival of mice transplanted with shPmi blast crisis CML relative to those transplanted with shScr cells (Figure 5E). In addition, total leukemia cell numbers from BM subjected to mannose were significantly reduced (Figure 5F). Similarly, the MLL-AF9 mouse model exhibited significantly prolonged survival when fed a mannose diet (Figure 5G). These results demonstrated that a mannose diet, alone or in combination with PMI inhibition, can suppress leukemia cell growth in a murine leukemia model.

3.5 | Mannose diet regulates the transcriptome of leukemia cell metabolism

To better understand how a mannose diet suppresses leukemia growth, and to assess the associated changes in gene expression, we performed RNA-seq on mannose diet-fed and normal diet-fed blast crisis CML model mice. Volcano plot and heatmap of RNA-seq data revealed that 10 genes were upregulated and 7 genes were downregulated by >2-fold in the mannose diet-fed mice compared with normal-fed mice (P < .05; Figure 6A,B). Gene set enrichment analysis was used to determine the extent to which metabolic target genes changed expression. Expression of genes involved in mitochondrial gene expression, mitochondrial function, and the TCA cycle was significantly reduced (Figure 6C,D). In addition, the variation in ribonucleoprotein-related genes was marked (Table S5). ¹³C₆-mannose metabolic flux analysis confirmed that mannose loading suppressed the TCA cycle (Figure 3A). In fact, XF analyzer analysis of leukemia cells collected from the BM of blast crisis CML mice and MLL-AF9 mice showed significantly decreased OCR and extracellular acidification rate (EACR) in the leukemia cells of the mannose diet-fed group (Figure 6E,F). Therefore, a mannose diet regulates the transcriptome of leukemia cell metabolism.

Furthermore, because excessive mannose loading resulted in the accumulation of mannose-6-phosphate, we examined the effect of mannose-6-phosphate on leukemia metabolism *in vitro*. First, a comparison of the OCRs of K562 cells cultured in glucose (10 mmol/L) with those of K562 cells cultured in mannose (10 mmol/L) showed that OXPHOS was significantly lower in K562 cells cultured in mannose (Figure S5A). Addition of mannose-6-phosphate to the medium at concentrations of 10, 20, and 50 mmol/L inhibited cell proliferation in a concentration-dependent manner (Figure S5B). Furthermore, mannose-6-phosphate addition inhibited OXPHOS and glycolysis (Figure S5C,D). These results demonstrated that excess mannose and mannose-6-phosphate suppressed OXPHOS and glycolysis.

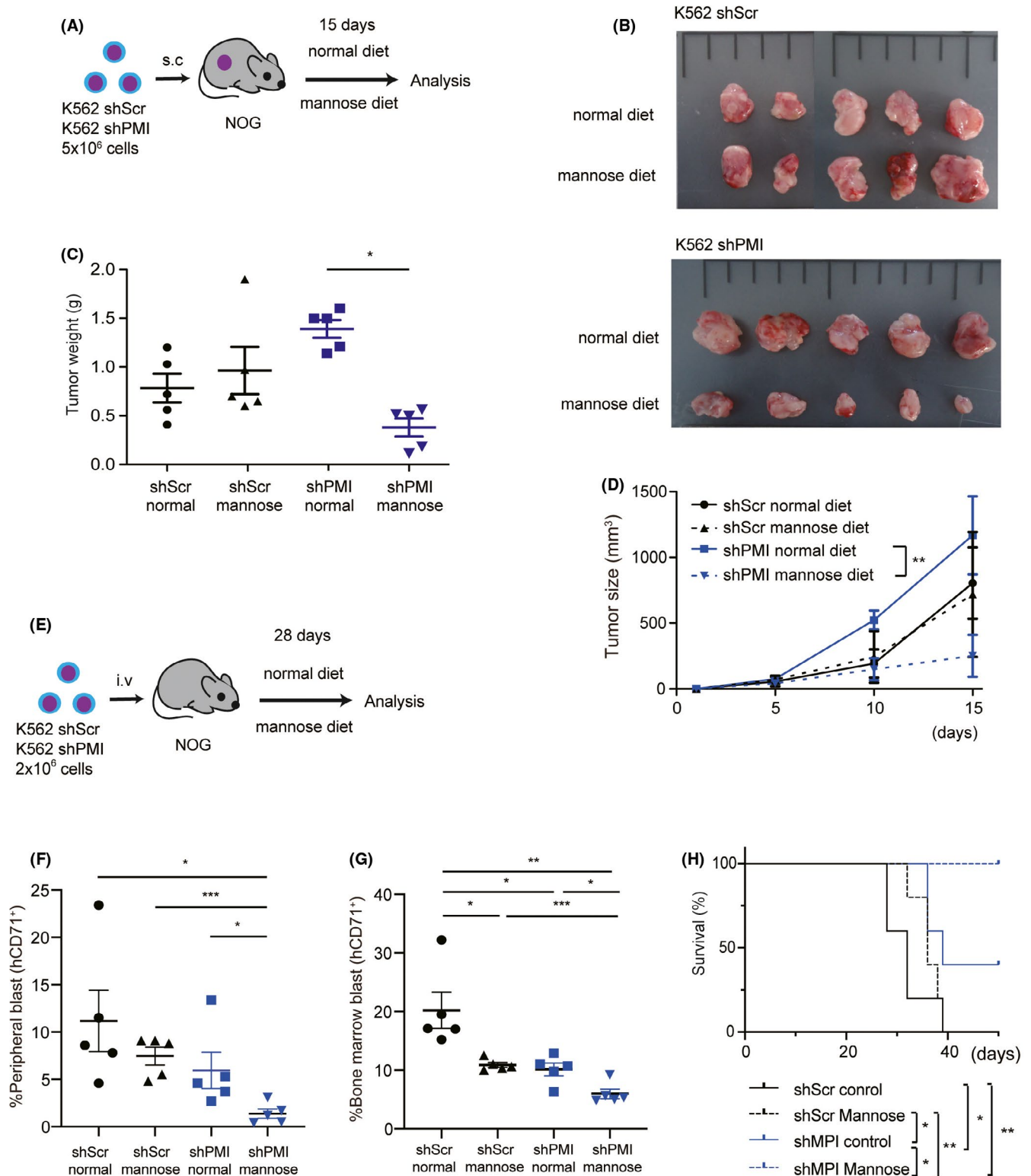


FIGURE 4 In vivo experiments in a xenograft leukemia mouse model demonstrate that mannose diet exceeding PMI capacity inhibits growth of leukemia cells. (A) Schematic outline of the subcutaneous K562 xenograft model fed a mannose diet. (B-D) Mannose diet significantly inhibited growth of K562 shPMI tumors (B). Tumor weight (C) and tumor size (D) ($n = 5$). (D) Data represent means \pm standard deviation. * $P < .05$; ** $P < .01$; *** $P < .001$ by two-way ANOVA. E, Schematic outline of the intravenous K562 model fed a mannose diet. (F, G) The mannose diet led to a significant reduction in the number of circulating CD71⁺ sh PMI K562 cells in peripheral blood (F) and bone marrow (G; $n = 5$). (H) The mannose diet extended the survival of shPMI K562 recipient mice significantly ($n = 5$). Significant differences in survival between cohorts was assessed by a log-rank test. * $P < .05$; ** $P < .01$; *** $P < .001$

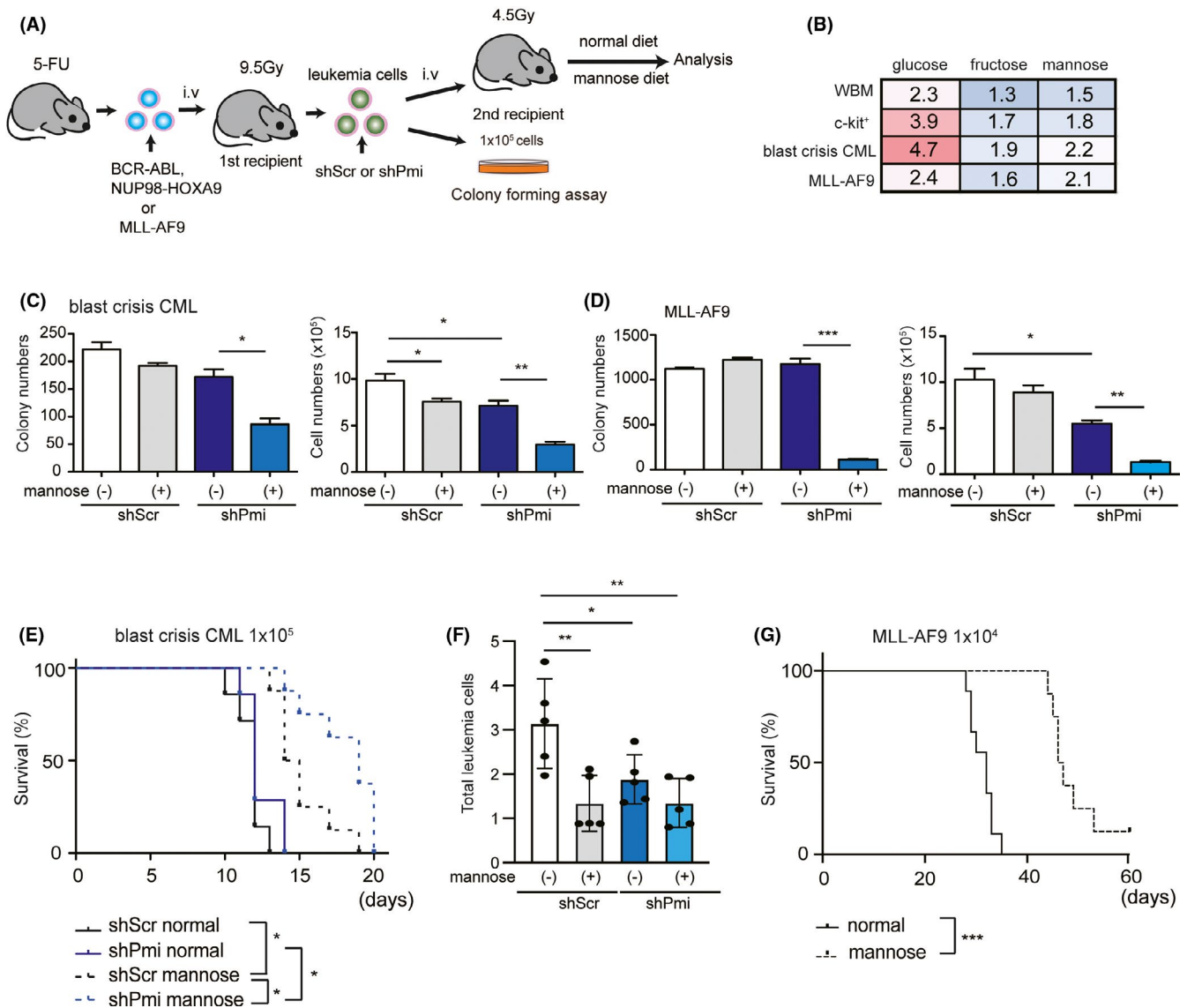


FIGURE 5 Combination treatment with mannose diet and PMI suppression exerts antileukemia activity ex vivo and in vivo in a leukemia mouse model. (A) Schematic outline of the blast crisis CML and MLL-AF9 mouse model. Blast crisis CML cells with shScr or shPmi were transplanted into sublethally irradiated mice. (B) Evaluation of glycolytic activity by mannose or fructose of normal whole bone marrow cells (WBM), c-kit⁺ fractions from normal bone marrow, blast crisis CML cells, and MLL-AF9 leukemia cells. (C, D) Leukemia cells infected with shScr or shPmi were cultured in methylcellulose medium with or without mannose. Graph shows the number of colonies and cell counts of blast crisis CML (C) and MLL-AF9 (D). Addition of mannose decreased cell proliferation, especially in shPmi. (E) Secondary recipients of 10⁵ blast crisis CML cells transduced with shScr or shPmi were fed a normal or mannose diet. Recipient mice fed mannose lived significantly longer, and survival was significantly extended when the mannose diet was combined with shPmi (shScr, normal diet, n = 7; shPmi, normal diet, n = 7; shScr, mannose diet, n = 8; shPmi, mannose diet, n = 8). (F) Mannose diet significantly decreased the total numbers of GFP⁺ leukemia cells (n = 5). (G) Secondary recipient mice of 10⁴ MLL-AF9 cells were fed a normal or mannose diet. Recipient mice fed mannose lived significantly longer (normal diet, n = 9, mannose diet, n = 8). The significance of differences in survival between cohorts was assessed by a log-rank test. *P < .05; **P < .01; ***P < .001

3.6 | PMI expression is a prognostic factor for myeloid leukemia

Finally, we analyzed the relevance of PMI expression to the survival of AML patients in previously published gene expression datasets. High expression of PMI in AML was significantly associated

with poorer prognosis in the 2 databases (Figure 7A; Prognoscan: GSE12417-GPL97, 7B: TCGA²⁵). Furthermore, in CML, MPI expression increased as stage progressed (Figure 7C; GSE4170).²⁶ Indeed, shPMI AML cells were more susceptible to anticancer drugs such as cytarabine, doxorubicin, and etoposide than control shScr cells (Figure 7D). These results indicated that PMI may be a useful target for the development of new metabolic therapies for leukemia.

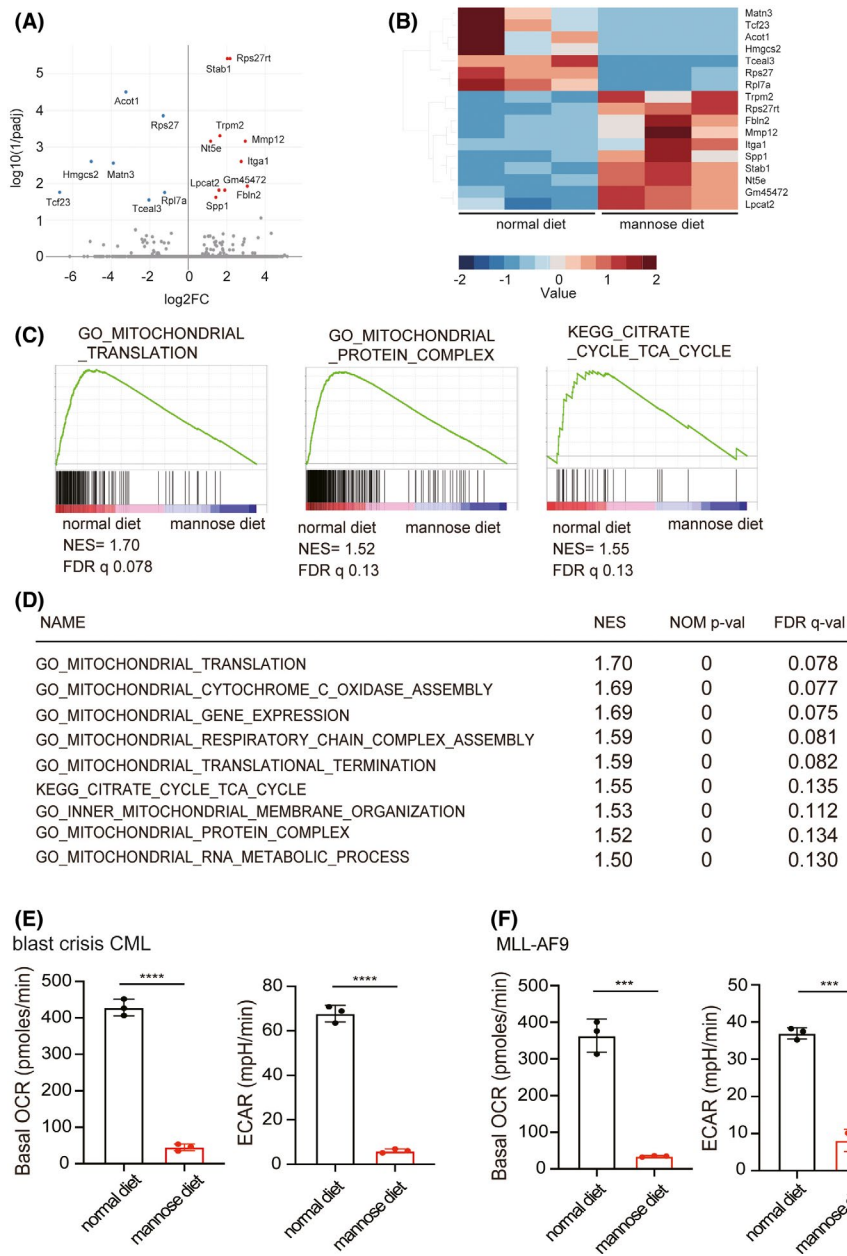


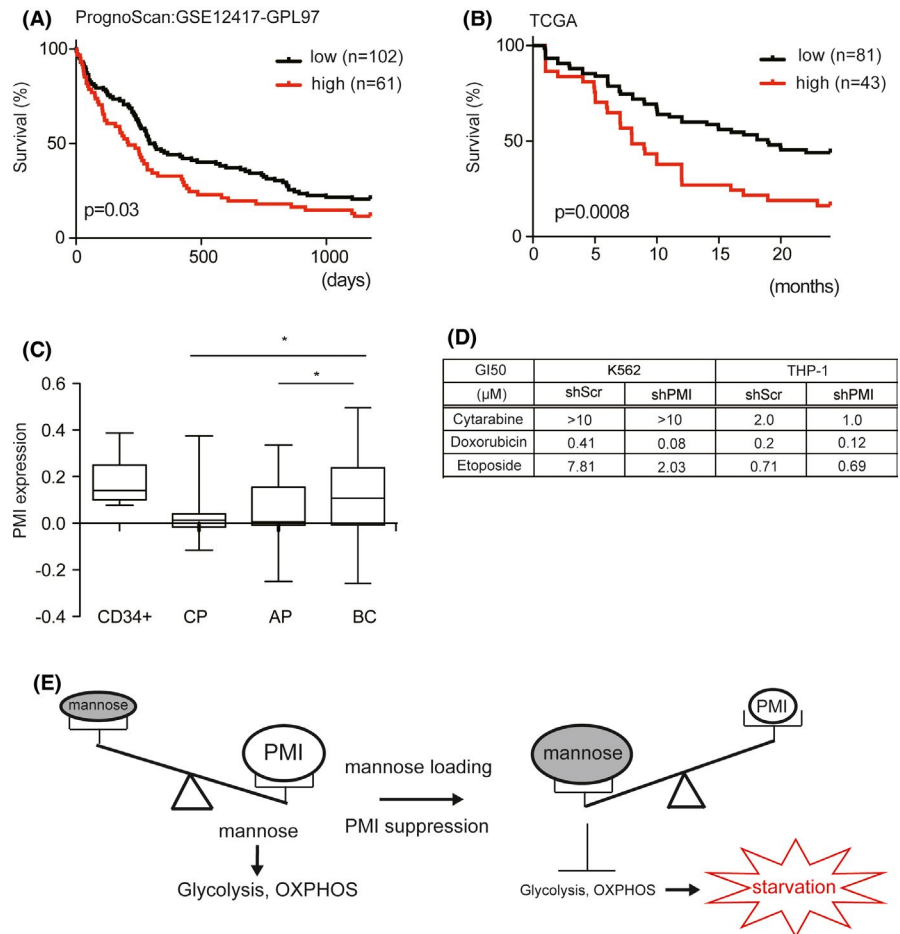
FIGURE 6 A mannose diet regulates the transcriptome of leukemia cell metabolism. (A, B) Leukemia cells were isolated from the bone marrow of blast crisis CML mice fed a normal or mannose diet, and gene expression was analyzed by RNA-seq ($n = 3$). Volcano plot (A) and heatmap (B) of RNA-seq data revealed 10 genes upregulated and 7 genes downregulated >2 -fold ($P < .05$). (C, D) Gene set enrichment analysis revealed reduced expression of genes involved in mitochondrial gene expression, mitochondrial function, and the TCA cycle in blast crisis CML cells from mice fed a mannose diet. (E, F) OCR and ECAR of mannose diet-fed leukemia cells of blast crisis CML mice (E) and MLL-AF9 mice (F) were significantly lower than those fed a normal diet

4 | DISCUSSION

Glucose consumption by leukemia cells decreases glucose levels in the BM, and it had previously been unclear whether these cells could use other carbohydrates as fuel for glycolysis. In this study, we used an extracellular flux analyzer to measure the glycolytic activity of leukemia cells toward various carbohydrates. We found that mannose and fructose could also serve as glycolytic energy sources. High expression of the fructose transporter GLUT5 is a prognostic factor for AML and has been explored as a novel therapeutic target.¹⁸ Our analysis also demonstrated that fructose can serve as an energy source for leukemia. Mannose is a monosaccharide that can enter cells through glucose transporters (GLUT1, GLUT2). Mannose is widely distributed in body fluids and tissues, especially in nerves, skin, testis, retina, liver, and intestine. It is

used to synthesize glycoproteins and also participates in immune regulation.²⁷ Because mannose is metabolized by the same enzymes that metabolize glucose, it interferes with glucose metabolism and inhibits cancer cell growth.¹³ In pancreatic cancer-derived xenografts, as well as in inflammation-driven and genetically engineered models of colorectal cancer, the disruption of glucose metabolism that results from mannose supplementation renders cancer cells more sensitive to chemotherapy-induced apoptosis.¹³ Recently, mannose was reported to be effective against lung cancer, breast cancer, and osteosarcoma.²⁸⁻³² Low expression of PMI makes cells more sensitive to the antitumor effect of mannose, and all of these cancers express low levels of PMI. By contrast, leukemia cells express PMI, but it remains unclear how mannose metabolism contributes to their survival and proliferation. Here, we demonstrated that PMI mobilizes mannose into the glycolytic

FIGURE 7 PMI expression is a prognostic factor for myeloid leukemia. (A, B) Kaplan-Meier survival curves of 2 cohorts of patients. Analysis by Prognoscan: GSE12417-GPL97 (A) and TCGA (B) showed that high expression of PMI predicted reduced overall survival and is a risk factor for poor prognosis in AML. (C) Expression of PMI increased significantly as the stage progressed to CP, AP, and BC in CML. (GSE4170) (D) K562 and THP-1 transduced with shScr and shPMI were treated with cytarabine, doxorubicin, and etoposide for 48 h. The growth inhibitory concentration 50 (GI50) was evaluated by nonlinear regression analysis using GraphPad Prism. (E) Schematic representation of the combination therapy for PMI suppression and mannose loading



system, TCA cycle, and PPP in leukemia cells, therefore providing an energy source during glucose starvation. Suppression of PMI expression in leukemia cells also resulted in the accumulation of mannose-6-phosphate due to mannose loading; a decrease in the levels of metabolites of the glycolytic system, TCA cycle, and PPP; and a marked suppression of cell proliferation. Surprisingly, we found that continuous loading of mannose via the diet changed the transcriptome of leukemia cells and suppressed mitochondrial metabolism. OXPHOS is involved in the resistance of leukemia cells to anticancer drugs,³³⁻³⁶ although a mannose diet can suppress OXPHOS at the level of transcription and metabolites. Mannose diet alone inhibited cancer growth in a leukemia mouse model, although it had no antileukemia effect in a cell line xenograft model. We speculate that the difference in the effects of a mannose diet was due to differences in glycolytic activity and glycolysis dependence between the cell lines and the leukemia mouse model. Because PMI is a prognostic factor for AML, the development of PMI inhibitors is essential for the use of mannose in the treatment of leukemia. MLS0315771 is reported to be a PMI inhibitor, although it exerted no clear antileukemia effect (data not shown).³⁷ In conclusion, mannose serves as a glycolytic energy source for leukemia cells during glucose starvation, but mannose that exceeds the processing capacity of PMI inhibits cell proliferation. The

combination of PMI suppression and mannose loading provides a new therapeutic approach to target leukemia energy metabolism (Figure 7E).

ACKNOWLEDGEMENTS

This research was supported by JSPS KAKENHI Grants (Numbers JP 18K16094, JP19K17367 and JP 20K08735), the Shinnihon Foundation of Advanced Medical Treatment Research, and the Japanese Society of Hematology Research.

DISCLOSURE

The authors declare no competing financial interests.

AUTHOR CONTRIBUTION

YS, MK, and AY, designed experiments, performed research, analyzed data, and wrote the manuscript with help from SK, LH; SK, MN, and SN provided human leukemia samples; TT and SY measured mannose concentration; and HM designed the experiments, analyzed the results, and wrote the manuscript.

ORCID

Yusuke Saito <https://orcid.org/0000-0002-4605-5635>

Hiroshi Moritake <https://orcid.org/0000-0001-5471-7646>

REFERENCES

1. Warburg O. On respiratory impairment in cancer cells. *Science*. 1956;124:269-270.
2. Shim H, Dolde C, Lewis BC, et al. c-Myc transactivation of LDH-A: implications for tumor metabolism and growth. *Proc Natl Acad Sci USA*. 1997;94:6658-6663.
3. Osthus RC, Shim H, Kim S, et al. Deregulation of glucose transporter 1 and glycolytic gene expression by c-Myc. *J Biol Chem*. 2000;275:21797-21800.
4. Gao P, Tchernyshyov I, Chang T-C, et al. c-Myc suppression of miR-23a/b enhances mitochondrial glutaminase expression and glutamine metabolism. *Nature*. 2009;458:762-765.
5. Morrish F, Noonan J, Perez-Olsen C, et al. Myc-dependent mitochondrial generation of acetyl-CoA contributes to fatty acid biosynthesis and histone acetylation during cell cycle entry. *J Biol Chem*. 2010;285:36267-36274.
6. Stieglitz E, Taylor-Weiner AN, Chang TY, et al. The genomic landscape of juvenile myelomonocytic leukemia. *Nat Genet*. 2015;47:1326-1333.
7. Roberts KG, Mullighan CG. Genomics in acute lymphoblastic leukaemia: insights and treatment implications. *Nat Rev Clin Oncol*. 2015;12:344-357.
8. Bullinger L, Döhner K, Döhner H. Genomics of acute myeloid leukemia diagnosis and pathways. *J Clin Oncol*. 2017;35:934-946.
9. Ying H, Kimmelman A, Lyssiotis C, et al. Oncogenic Kras maintains pancreatic tumors through regulation of anabolic glucose metabolism. *Cell*. 2012;149:656-670.
10. Wang Y-H, Israelsen W, Lee D, et al. Cell-state-specific metabolic dependency in hematopoiesis and leukemogenesis. *Cell*. 2014;158:1309-1323.
11. Tiziani S, Kang Y, Harjanto R, et al. Metabolomics of the tumor microenvironment in pediatric acute lymphoblastic leukemia. *PLoS One*. 2013;8:e82859.
12. Echeverría C, Nualart F, Ferrada L, Smith GJ, Godoy AS. Hexose transporters in cancer: from multifunctionality to diagnosis and therapy. *Trends Endocrinol Metab*. 2021;32:198-211.
13. Gonzalez PS, O'Prey J, Cardaci S, et al. Mannose impairs tumour growth and enhances chemotherapy. *Nature*. 2018;563:719-723.
14. Saito Y, Kaneda K, Suekane A, et al. Maintenance of the hematopoietic stem cell pool in bone marrow niches by EVI1-regulated GPR56. *Leukemia*. 2013;27:1637-1649.
15. Saito Y, Nakahata S, Yamakawa N, et al. CD52 as a molecular target for immunotherapy to treat acute myeloid leukemia with high EVI1 expression. *Leukemia*. 2011;25:921-931.
16. Miwa I, Taguchi T. A simple HPLC assay for plasma D-mannose. *Clin Chim Acta*. 2015;422:42-43.
17. Saito Y, Chapple RH, Lin A, Kitano A, Nakada D. AMPK protects leukemia-initiating cells in myeloid leukemias from metabolic stress in the bone marrow. *Cell Stem Cell*. 2015;17:585-596.
18. Chen W-L, Wang Y-Y, Zhao A, et al. Enhanced fructose utilization mediated by SLC2A5 is a unique metabolic feature of acute myeloid leukemia with therapeutic potential. *Cancer Cell*. 2016;30:779-791.
19. Jeong S, Savino AM, Chirayil R, et al. High fructose drives the serine synthesis pathway in acute myeloid leukemic cells. *Cell Metab*. 2021;33:145-159.e146.
20. Krause N, Wegner A. Fructose metabolism in cancer. *Cells*. 2020;9:2635.
21. Zhang D, Chia C, Jiao X, et al. D-mannose induces regulatory T cells and suppresses immunopathology. *Nat Med*. 2017;23:1036-1045.
22. Torretta S, Scagliola A, Ricci L, et al. D-mannose suppresses macrophage IL-1 β production. *Nat Commun*. 2020;11:6343.
23. Dash AB, Williams IR, Kutok JL, et al. A murine model of CML blast crisis induced by cooperation between BCR/ABL and NUP98/HOXA9. *Proc Natl Acad Sci USA*. 2002;99:7622-7627.
24. Somerville TC, Cleary ML. Identification and characterization of leukemia stem cells in murine MLL-AF9 acute myeloid leukemia. *Cancer Cell*. 2006;10:257-268.
25. Ley TJ, Miller C, Ding L, et al. Genomic and epigenomic landscapes of adult de novo acute myeloid leukemia. *N Engl J Med*. 2013;368:2059-2074.
26. Radich JP, Dai H, Mao M, et al. Gene expression changes associated with progression and response in chronic myeloid leukemia. *Proc Natl Acad Sci USA*. 2006;103:2794-2799.
27. Wei Z, Huang L, Cui L, Zhu X. Mannose: good player and assister in pharmacotherapy. *Biomed Pharmacother*. 2020;129:110420.
28. Fang Z, Wang R, Zhao H, Yao H, Ouyang J, Zhang X. Mannose promotes metabolic discrimination of osteosarcoma cells at single-cell level by mass spectrometry. *Anal Chem*. 2020;92:2690-2696.
29. Gautam L, Sharma R, Shrivastava P, Vyas S, Vyas SP. Development and characterization of biocompatible mannose functionalized mesospheres: an effective chemotherapeutic approach for lung cancer targeting. *AAPS PharmSciTech*. 2020;21:190.
30. Liu F, Xu X, Li C, et al. Mannose synergizes with chemoradiotherapy to cure cancer via metabolically targeting HIF-1 in a novel triple-negative glioblastoma mouse model. *Clin Transl Med*. 2020;10:e226.
31. Sha J, Cao D, Cui R, et al. Mannose impairs lung adenocarcinoma growth and enhances the sensitivity of A549 cells to carboplatin. *Cancer Manag Res*. 2020;12:11077-11083.
32. Wang Y, Xie S, He B. Mannose shows antitumour properties against lung cancer via inhibiting proliferation, promoting cisplatin-mediated apoptosis and reducing metastasis. *Mol Med Rep*. 2020;22:2957-2965.
33. Lagadinou E, Sach A, Callahan K, et al. BCL-2 inhibition targets oxidative phosphorylation and selectively eradicates quiescent human leukemia stem cells. *Cell Stem Cell*. 2013;12:329-341.
34. Farge T, Saland E, de Toni F, et al. Chemotherapy-resistant human acute myeloid leukemia cells are not enriched for leukemic stem cells but require oxidative metabolism. *Cancer Discov*. 2017;7(7):716-735.
35. Kuntz EM, Baquero P, Michie AM, et al. Targeting mitochondrial oxidative phosphorylation eradicates therapy-resistant chronic myeloid leukemia stem cells. *Nat Med*. 2017;23:1234-1240.
36. Saito Y, Sawa D, Kinoshita M, et al. EVI1 triggers metabolic reprogramming associated with leukemogenesis and increases sensitivity to L-asparaginase. *Haematologica*. 2020;105:2118-2129.
37. Sharma V, Ichikawa M, He P, et al. Phosphomannose isomerase inhibitors improve N-glycosylation in selected phosphomannomutase-deficient fibroblasts. *J Biol Chem*. 2011;286:39431-39438.

SUPPORTING INFORMATION

Additional supporting information may be found in the online version of the article at the publisher's website.

How to cite this article: Saito Y, Kinoshita M, Yamada A, et al. Mannose and phosphomannose isomerase regulate energy metabolism under glucose starvation in leukemia. *Cancer Sci*. 2021;112:4944-4956. doi:[10.1111/cas.15138](https://doi.org/10.1111/cas.15138)